IEEE Journal of Microwaves

Received 14 June 2024; revised 6 September 2024; accepted 15 October 2024. Date of publication 6 November 2024; date of current version 2 December 2024.

Digital Object Identifier 10.1109/JMW.2024.3484754

Time-Transient Wireless RF Sensor With Differentiative Detection Capability in Ionic Aqueous Environment for Water Conservation and Green Cleaning

SOBHAN GHOLAMI [1], EMRE UNAL [1], AND HILMI VOLKAN DEMIR [1,2] (Fellow, IEEE)

(Invited Paper)

[1]Department of Electrical and Electronics Engineering, Department of Physics, UNAM – Institute of Materials Science and Nanotechnology and The National Nanotechnology Research Center, Bilkent University, 06800 Ankara, Türkiye

[2]Luminous! Center of Excellence for Semiconductor Lighting and Displays, School of Electrical and Electronic Engineering, Division of Physics and Applied Physics, School of Physical and Mathematical Sciences, School of Materials Science and Engineering, Nanyang Technological University, Singapore 639798

CORRESPONDING AUTHOR: Hilmi Volkan Demir (e-mail: volkan@bilkent.edu.tr).

The work of Hilmi Volkan Demir was supported by TUBA and TUBITAK 2247-A National Leader Researchers Program under Grant 121C266. This work was supported by TUBITAK's Industry Innovation Network Mechanism (SAYEM) Program under Grant 121D010 (Akıllı Ev Platformu) in collaboration with Eczacıbaşı.

ABSTRACT A novel wireless microstrip-based RF sensor designed for detecting changes in the ionic content of water and the addition of solid contaminant objects is proposed and demonstrated for the purpose of water conservation and green cleaning. The sensor can be installed on the exterior wall of dielectric containers and customized according to the material of the container (such as porcelain) to enable wireless sensing inside the container. Its operation within the lower microwave frequency range (670–730 MHz) serves to minimize signal attenuation in water and streamline circuitry design. The most significant feature of this sensor is its unique design, rendering it impervious to its surrounding environment. This not only shields it from environmental noise but also maximizes its sensitivity by efficiently utilizing incoming power for sensing purposes. The sensor exhibits remarkable sensitivity, capable of detecting solute concentrations as low as 3.125×10^{-3} M in water inside the container. It can also detect the insertion of foreign solid objects into the container from the exterior wirelessly and distinguish them from liquids being added. As a proof-of-concept demonstration, the sensor in this study was built for a porcelain wall of 10-12 mm thickness. The sensor's small size and the materials used for its fabrication make it an ideal choice for various smart bathroom applications, where accurate and reliable water use monitoring is essential for efficient water conservation and green cleaning. The sensor's ability to distinguish between the added solid objects and liquid electrolytes in the container provides the necessary sensing data for running water-saving and efficient washing mechanisms in bathrooms.

INDEX TERMS Chemical and biological sensors, green cleaning, microwave propagation, microwave sensors, microwaves in climate change, signal analysis, water conservation, water monitoring.

I. INTRODUCTION

In recent years, the pressing issue of global warming and its effect on water resources [1], [2], [3], has attracted much attention in using technology for water conservation. There have been efforts in the reduction of water use, especially in bathrooms, as a significant source of water consumption at homes by imposing regulations [4]. In addition, new toilet designs have been introduced that require less water for flushing [5], [6]. Sensors have also been employed to promote water-conserving practices in bathroom facilities. Examples of such sensors are IR proximity sensors for automatic urinal flushing in public bathrooms, as well as load detectors installed under toilet lids for automatic flushing [7], [8].

While IR sensors activate the flushing mechanism based on the reflection of electromagnetic wave (EMW) of a specific wavelength from the presence of an object or person in front of the sensor, in load sensors, mechanical energy is converted into electrical signals to show the presence of a person sitting on the lid and obviate the need to mechanically press the flush button or press it multiple times unnecessarily after standing up. Yet non operates based on the actual presence of excreta in the toilet.

For developing a sensor that senses the presence of excreta in the toilet, it is important to consider all sanitation issues regarding the operation and maintenance of such sensors. This calls for a contactless mechanism of sensing that ensures the separation between the sensor and excreta. Waves can travel through different mediums and perform the sensing operation without any physical contact between the source and the material under test. EMWs being able to travel through both porcelain and water and utilizing cheaper equipment are a better option compared to other waves like ultrasound which require more complex hardware. EMWs do not require physical contact with human excreta and thus minimize unwanted contamination. A considerable number of research studies have been conducted in microwave frequencies and demonstrated the potential of microwave devices being employed as sensors [9], [10], [11] [12], [13], [14]. These sensors have been demonstrated to detect alterations in the electromagnetic properties of a wide range of materials. They employ reflection, reflection/transmission, and resonance perturbation measurement methods to achieve sensing in the framework of 1 and/or 2 port networks. Nevertheless, a significant proportion of these sensors rely on direct contact between the material under test (MUT) and the sensor. This was observed using open-ended coax cables [15], [16], [17], or microstrip resonators [18], [19], [20]. Research has also been conducted into confining the MUT in microfluid tubes to isolate the MUT; however, the restricted size of the tubes and delicate operation of the sensors limit their applications in a bathroom environment [21], [22], [23].

Antennas, in some cases, were utilized to discern the variations in the electromagnetic properties of materials from the transmission information [24], [25], [26]. Still, the application of antennas as a sensing mechanism is only effective when the MUT is completely separated, which does not seem feasible in a restroom environment where various variable elements exist. The reflection response of an antenna has been used for determining concentrations of sugar and salt in water in [27] where the antenna was operated as a resonator and immersed in the solution under test. In [28], [29], an ultra-high-quality factor resonator was shown. The mentioned resonator is capable of distinguishing between different liquids inside a tube submerged in water in the near field, primarily due to its exceptionally large quality factor. However, this was only presented for the cases where the layer used between the resonator and the MUT was extremely thin to allow the field to penetrate inside. A two-port microstrip resonator was introduced in [30] capable of detecting different layers of materials

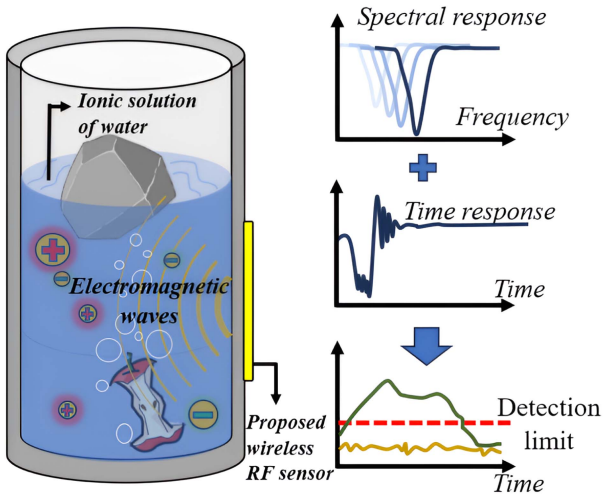

FIGURE 1. Conceptual illustration of wireless RF sensing in time-transient mode operated in ionic aqueous environment.

(mainly for oil and sand) wirelessly based on variations in the transmission response of the resonator, employed to make out the difference in the state of materials under test. One drawback in such sensors is that the electromagnetic wave does not propagate inside the medium, making them unsuitable for detecting objects located farther inside the medium.

This paper presents a novel time-dependent single-frequency sensor design capable of detecting changes in the concentration and presence of dielectric objects within water inside a porcelain container. This capability has the potential to play a distinct role in determining the necessary amount of water for each flushing, thereby preventing the waste of water from excessive flushing in toilets. The operational frequency of the sensor is carefully selected to minimize the loss due to the attenuation of electromagnetic waves while also ensuring that the wavelength is comparable to the size of the objects inserted into the water to carry out detection.

The unique characteristics of this design allow it to be installed on the outer surface of a toilet and perform sensing without being exposed to human excreta. Moreover, the distinctive design of this resonator renders it completely uncoupled from its surroundings, establishing a sensing environment where the only variables are confined within the toilet. Additionally, this design is compact in size, making it compatible with existing toilet setups. A conceptual representation of the sensor and its operation is depicted in Fig. 1.

II. DESIGN OF THE PROPOSED SENSOR

The sensor's desired characteristics pose a significant challenge in the design process. Achieving the right balance between size, directivity, conformity, and operating frequency is a formidable obstacle. Microstrip patch configurations, with their inherent qualities of conformity, low profile, and versatility, emerge as the optimal choice for sensor design. Moreover, by employing tunable microstrip patch antenna structures for

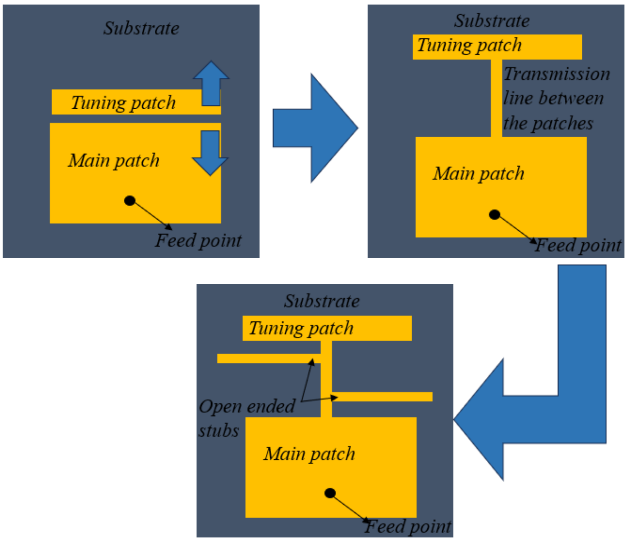

FIGURE 2. Sensor design steps.

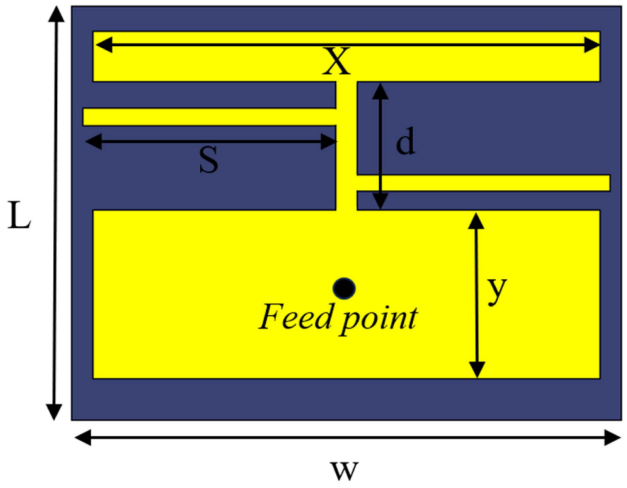

FIGURE 3. Proposed sensor's structure. W=65 mm, L=50 mm, d= 15.2 mm S= 30 mm, x=60 mm, y=23 mm.

the sensor, it would be possible to tune the resonance frequency of the design. In some designs, varactors are placed between the main and tuning patch to provide a varying LC element to tune the frequency [31]. However, the integration of varactors in the design introduces additional DC circuitry demands, further complicating the final product— an aspect that is less desirable.

To lower the resonance frequency while maintaining directivity, we strategically incorporate capacitive elements between the main patch and the tuning patch, as shown in Fig. 2. In this design, open-ended microstrip transmission lines, also referred to as stubs, are positioned along another transmission line connecting the main patch to the tuning patch. These stubs are optimized to serve as capacitive elements.

According to the two-port model of a terminated transmission line, looking into a transmission line toward the load, the input impedance [32] is:

$$Z_{in} = Z_0 \frac{Z_L + jZ_0 \tan \beta l}{Z_0 + jZ_L \tan \beta l} \tag{1}$$

where Z_0 represent the intrinsic impedance of the line, Z_L the terminating load and l, the length of the line.

Setting $Z_L = \infty$ for an open-ended transmission line makes:

$$Z_{in} = -jZ_0 \cot \beta l \tag{2}$$

According to (2), the open-ended transmission line can provide almost any reactance by tuning the length and the intrinsic impedance of the line. The intrinsic impedance of the line is determined using [33] :

$$Z_0 = \frac{120\pi}{\sqrt{\epsilon_{eff}}\left[\frac{w}{h} + 1.393 + 0.667\ln\left(\frac{w}{h} + 1.44\right)\right]} \tag{3}$$

$$\epsilon_{eff} = \frac{\epsilon_r + 1}{2} + \frac{\epsilon_r - 1}{2}\left[1 + 12\frac{h}{w}\right]^{-1/2} \tag{4}$$

In (3) and (4), w is the width of the stub; h is the height of the underlying dielectric substrate and ϵ_r is the relative dielectric constant of the substrate.

To implement the stubs, a 50-ohm microstrip transmission line was drawn between the patch and the tuning patch. Two open-ended stubs were introduced on both sides of the line to provide capacitance. The location of the stubs from the tuning patch, their length, and length of the transmission line were tuned using Computer Simulation Technology Microwave Studio to achieve the lowest resonant frequency possible. The sensor was designed on Rogers Corporations RT5880 double-sided copper with a dielectric thickness of 0.79 mm and copper thickness of 0.018 mm shown in Fig. 3.

As the sensor's primary objective is to transmit EMW through porcelain into water, the tuning and optimization process was conducted within a porcelain medium immersed in water. This approach closely emulates the sensor's real operational conditions. By adopting this optimization method, reflections from the sensor/porcelain interface were minimized, allowing a higher proportion of the source power to penetrate the medium and facilitate sensing. Porcelain in the numerical simulation is selected from the materials library of CST Microwave Studio 2019 with relative dielectric permittivity (ϵ_r) of 4.9 and electrical conductivity (σ) of 1×10^{-15} S/m. Fig. 4 visually represents the numerical simulation of the electric field radiated by the sensor into the medium, demonstrating the sensor's ability to remain isolated from its surrounding environment—a key accomplishment sought in our design.

The design was physically realized on a double-sided copper laminate of Rogers Corporations RT5880 (with $\epsilon_r = 2.2$ and $\tan\delta = 0.009$). Experimental testing was carried out on a porcelain container with a thickness between 10 to 12 mm. A comparison between numerical simulations and measurement

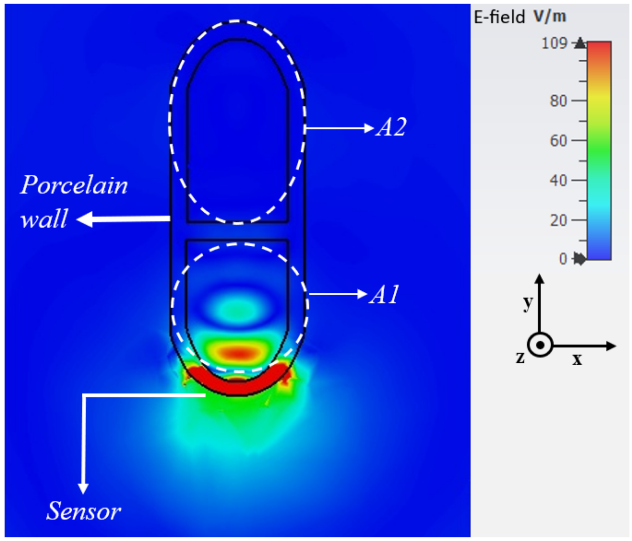

FIGURE 4. Z-cut representation of propagation of EMW through porcelain into water. A1 is the front side of the S pipe underneath the toilet bowl, where the excreta are first inserted. A2 is in the outgoing part of the S pipe.

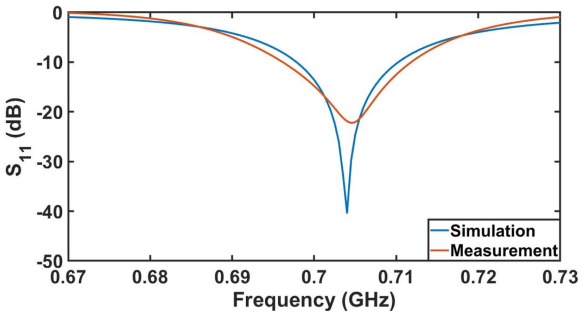

FIGURE 5. Experimentally measured reflection coefficient compared to numerical solution of the fabricated sensor.

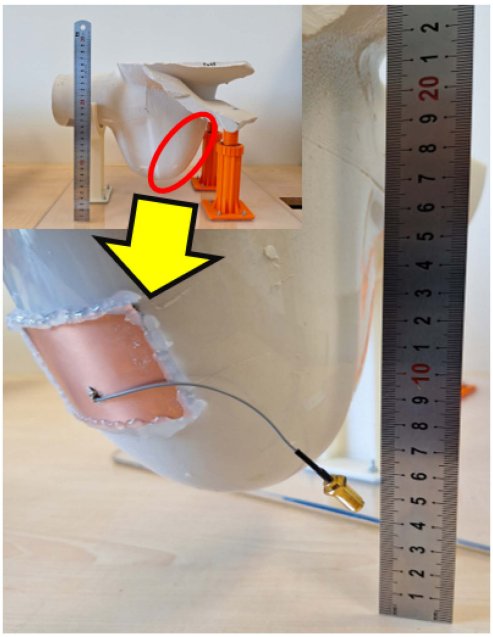

FIGURE 6. The modified toilet setup with a close look on how and where the sensor is installed.

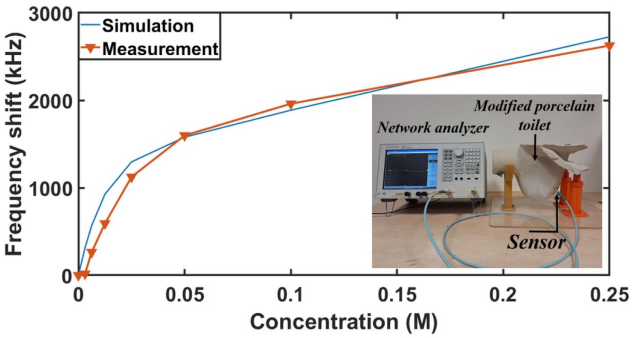

FIGURE 7. Comparing measurement and numerical results for the frequency shift corresponding to varying concentrations of NaCl in the measurement setup in the inset of the graph.

results is presented in Fig. 5 where the difference between resonance frequencies in measurement and simulation is less than 600 kHz.

III. RESULTS AND DISCUSSION

The proposed sensor is capable of detecting the change in the concentration of water and sense the insertion of dielectric objects in the toilet. To evaluate the capability of the designed sensor for practical application, a special structure is designed to emulate the actual situation in a bathroom. The sensor is hot glued to the front section of the S pipe on the bottom of the porcelain toilet setup shown in Fig. 6. The sensor communicates with an Agilent technologies E5061B ENA through an SMA cable shown in the inset of Fig. 7. Careful attention was given to thoroughly remove all air gaps between the sensor and the porcelain to prevent multiple reflections between the two surfaces.

To test the sensor and determine its sensing range in response to changes in the ionic content of water, we prepared samples of NaCl solutions with different concentrations in the range of 3.125×10^{-3} to 5.000×10^{-1} M (mol/L) using 99.9% pure NaCl. Additionally, we prepared an artificial urine solution following the formulation provided in [34] and maintained it at 37 °C. This allowed us to determine which concentrations of NaCl solutions at room temperature yield an equivalent electrical response when added to water instead of artificial urine.

To emulate the addition of feces to the medium, samples were prepared using the formulation in [35] with lengths of 65 – 67 mm and diameters of 25 – 27 mm.

A. DETECTING THE CHANGES IN IONIC CONCENTRATION OF WATER

The electrical response of a material to the incident electromagnetic wave is determined by its dielectric constant. The dielectric constant of pure water is well described by Debye model as a function of the frequency [36]:

$$\epsilon_w(f) = \epsilon_w(\infty) + \frac{\epsilon_w(0) - \epsilon_w(\infty)}{1 + i2\pi f \tau_w} \quad (5)$$

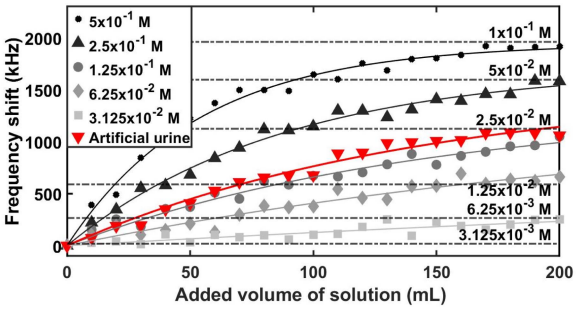

FIGURE 8. Measurement results of changes in resonance frequency (frequency shift) with respect to the volume of added NaCl solution with different concentrations. Horizontal dashed lines show the frequency shift corresponding to concentration of the mixture inside the toilet.

where $\epsilon_w(\infty)$ is the dielectric constant of water at a very high frequency, $\epsilon_w(0)$ is the dielectric constant of water at DC and τ_w is the relaxation time of pure water. Since (5) spans a broad frequency spectrum, it is reasonable to assume that the dielectric constant of water remains constant within the operational frequency range of this work (670-730 MHz).

When ions are dissolved in pure water, the DC dielectric constant of water and relaxation time are influenced by the presence of ions, resulting in modifications to the relation described in (5) [37]:

$$\epsilon_s(f) = \epsilon_w(\infty) + \frac{\epsilon_s(0) - \epsilon_w(\infty)}{1 + i2\pi f \tau_s} - i\frac{\delta}{2\pi f \epsilon_0} \tag{6}$$

Here ϵ_0 is the dielectric permittivity of free space, ϵ_s is the static dielectric constant, τ_s is the relaxation time, and δ is the conductivity of the resultant solution, which are functions of the concentration of the dissolved ions. Detailed relationships governing these properties can be found in [37], [38], [39].The introduction of an ionic solution with a concentration higher than that of water alters the ion content of the water, leading to changes in ϵ_s. These changes manifest as variations in the electrical response of the solution which in the case of this study, is the changes in the frequency of the minimum reflection coefficient (S11).

To examine changes in the sensor's steady-state reflection coefficient, the toilet bowl was filled with water containing varying concentrations of NaCl. We analyzed the resulting resonance frequency shift ($f - f_0$) concerning the baseline case when the medium consisted of only water (f_0). These comparisons are visually represented in Fig. 7. It is seen that the increase in the ion content of the medium leads to a consistent shift in the resonance frequency.

In the next step to observe the transient sensor response to the addition of ions, 200 mL volumes of solutions with concentrations of 3.125×10^{-2}, 6.250×10^{-2}, 1.250×10^{-1}, 2.500×10^{-1}, 5.000×10^{-1} M, and artificial urine were slowly injected into the test toilet setup, simulating the introduction of urine into the medium. Fig. 8. shows the shifts in the frequency *vs* volume of added solution for different solution concentrations. Horizontal dashed lines show the final concentration of the medium and the corresponding frequency shift based on prior measurements. Step by step, as more solution was added to the medium while the volume was constant-due to the physical nature of the S pipe at the bottom of the bowl-, the shift in the frequency monotonously increased.

Naturally when electrolyte is added to the medium where the concentration of electrolyte is very low, a considerable frequency shift entail. Since the volume is constant, as the electrolyte is added and more liquid is discharged from the other side of the S-pipe, more ion is also discharged with water. Therefore, the system approaches a limit with a pace that is very similar to natural logarithmic growth. As a result, we fitted the data points using:

$$\Delta f = a\left(1 - e^{-bv}\right) \tag{7}$$

Here a represents the maximum frequency shift expected to occur in the steady state and b determines the rate at which the steady state is reached. v is the volume of solution in mL added.

B. SIMULTANEOUSLY DETECTION OF THE ADDITION OF SOLID OBJECTS INTO WATER IN CONTRAST TO THE IONIC SOLUTION

The introduction of solid objects into a medium, when compared to the addition of solutions, often leads to significant and erratic shifts in resonance frequencies. Therefore, the transient response becomes a crucial aspect to consider. In the context of our study, when a solid object is introduced into the water, it generates ripples on the water's surface, with the amplitude of these ripples directly reflecting the energy associated with the inserted object. Consequently, analyzing the amplitude of these ripples serves as a valuable means of determining the presence of feces within the toilet. The sensor, loaded with water in design, captures and registers the ripples produced, which, in turn, induces direct changes in its resonance frequency. As a consequence, these ripples manifest as distinctive features on the frequency shift curve over time. Analyzing the frequency content of this time-dependent frequency shift curve offers distinctive features to differentiate feces from ionic solution.

We performed an instantaneous differential operation on the frequency shift data to isolate the ripples from the frequency shift curve. This operation effectively eliminates any influence from solid objects within the sensor's electromagnetic field. Following this step, we employ Fourier transformation to obtain the frequency components within the derivative of the frequency shift curve.

For the Fourier analysis, it is important to consider the sampling time of the signal. In our study, we set a consistent sampling time of 110 ms between each data point. Fig. 9 illustrates the three critical stages of detecting, analyzing, and comparing the ripples in the solid object insertion case together with the liquid injection case. For the most comprehensive examination, we conducted tests involving liquid injection from a height of 80 cm above the water level at a rate of 17 mL/s [40]. In Fig. 9(a), we present the frequency

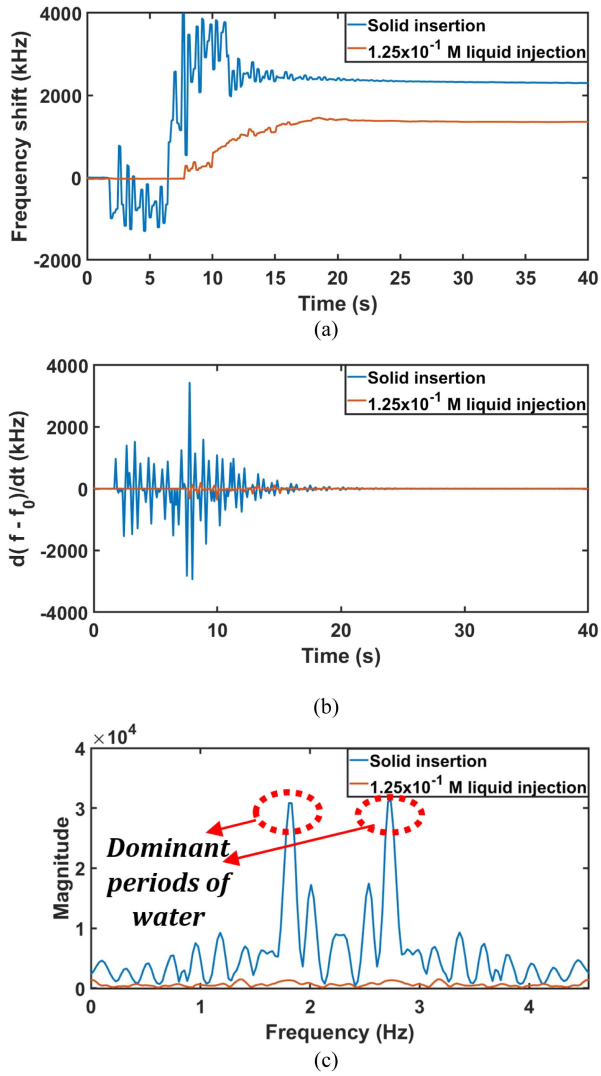

FIGURE 9. Measurement and analysis of injection of 1.25 × 10^{-1} M solution with insertion of solids into the medium: (a) frequency shift curves corresponding to both cases, (b) derivative of the frequency shift curves in both cases, and (c) frequency content of the derivative of frequency shift curve.

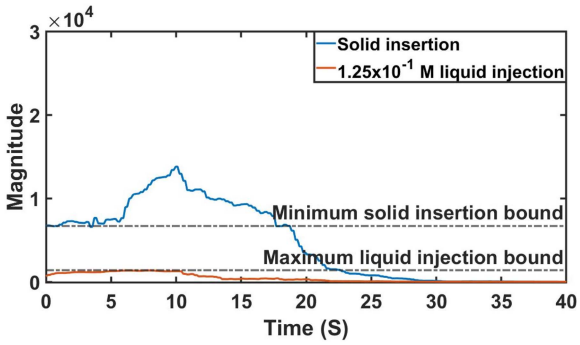

FIGURE 10. Comparing minimum and maximum detected sensing signal magnitude of solid insertion and 1.25 × 10^{-1} M NaCl solution injection.

shift curve resulting from the introduction of three 50-gram pieces of artificial feces compared with an injection of 220 mL of 1.25 × 10^{-1} M solution of NaCl. Fig. 9(b) showcases the derivative of the frequency shift curve ($\frac{d(f-f_0)}{dt}$) for both these cases, and in Fig. 9(c), we present the Fourier transform of the frequency shift curves. Two prominent frequency peaks within the range of 1.6 to 3.0 Hz are observed in our analysis of the solid insertion case. These peaks correspond to the dominant period of water ripples due to the depth of water in the toilet [41]. Significantly, these peaks consistently show up with noticeable magnitudes whenever a solid object is introduced into the water.

As it is expected (Fig. 9(c)) ripples generated by the injection of liquids into the toilet exhibit substantially smaller magnitudes within the modulation frequency range of 1.6 to 3.0 Hz compared to instances involving solid object insertion. Naturally, feces displace greater amounts of water leading to higher amplitudes of waves formed on the surface. This allows us to differentiate between the insertion of feces and urine into the toilet by analyzing the spectrum of the filtered data shown in Fig. 9(b). We achieve this by applying a bandpass filter and conducting spectral analysis on the frequency content of the derivative curve, ($\frac{d(f-f_0)}{dt}$), at regular time intervals. Following this approach also enables us to track the magnitude of the peaks within the 1.6 – 3.0 Hz range over time.

In Fig. 10, we selected the scenario with the lowest magnitude out of 9 tests for solid insertion and compared it to the injection case where the highest magnitude was reached. This comparison reveals a significant difference between these two extreme scenarios, underscoring the reliability of this analysis method in distinguishing between the incoming feces and urine in the toilet.

Table 1 demonstrates a quantitative comparison between the available characterization approaches and the sensor proposed in this work for operation in a bathroom environment. The fact that the sensor operates under 1 GHz with only 1 port-simplifies the required circuitry-as a determining factor in the large-scale employment of this design. Furthermore, coupling of the sensor with the medium and the design process followed with this goal renders it insensitive to the surrounding and enables it to focus only on the medium of interest for any alterations. As a result, what happens outside the toilet bowl does not affect the sensor response.

In this case study, the sensing algorithm is structured as follows: initially, the system performs the derivative and fft operation on the received frequency shift data to identify the presence of solid insertions. Upon detection of solid insertion, the washing procedure to flush the solid excreta is executed using the maximum amount of water available in the tank. The performed washing also removes any potential ionic solutions and the sensor will discard inputs during the washing procedure. In instances where no solid insertions are detected, the system shifts its focus to analyzing the resonance frequency's shift, specifically corresponding to the introduction of electrolytes which require substantially less amount of water for flushing compared to the solid detection case. This analytical approach enables the system to discern the concentration of the added solution, empowering it with the capability to execute programmable actions commensurate

TABLE 1. Comparison Between the Proposed Sensor and the Currently Available Microwave Solutions for Ionic Concentration Detection

	Our wireless RF sensor	Direct contact probes	Planar microstrip resonators	Planar high-quality factor microwave resonators	Free space measurement
Operational range (GHz)	0.67 - 0.72	0.5 - 20	1.5 - 5	1.5 - 2.5	1 - 4.5
Number of ports	1	1	2	2	2
Sensitivity to surrounding	low	low	low	low	high
Wireless sensing from the exterior	possible	not possible	requires sample holder	requires sample holder	possible

with the concentration level and dispensing water according to the concentration of injected liquid.

The application of this system can play an important role in wastewater management and water conservation through efficient resource allocation. Although some toilet setups come with dual flush capability (3-liter half-flush and 6-liter full-flush) [42] the extent to which this feature is used depends on the bathroom goers and in public toilets can lead to many mis-flushing. Considering each person on average visits the bathroom 6-7 times a day [43] (42 times a week on average) for urination and 3 times a day to 3 times a week for bowel movement [44], there is the possibility of 39 to 21 mis-flushing a week per person. Taking the difference in each mis-flush to be 3 liters, and at best case scenario only 10% of bathroom goers press the full-flush instead of half-flush, 6.3 to 11.7 liters of water per person per week is wasted. This adds up to a significant value once the total number of people visiting public bathrooms in public places like parks and shopping malls is considered. The proposed sensor automatically determines whether full or half flush is needed and prevents all the over-flushing cases. In addition, once toilet cisterns capable of flushing water in volumes more than only half and full-tank settings are developed, the sensor can fully employ its concentration detection capability and flush according to the amount of urine found in the bowl to save water beyond the 3-liter half-flush.

IV. CONCLUSION

A novel wireless sensor design capable of distinctly detecting changes in the ionic content of water and the insertion of solid objects that create ripples on the water surface in a dielectric container is introduced. The sensor detects changes as low as 3.125×10^{-3} M in the ionic content of water and distinguishes between the responses related to the alteration in the concentration of water and the insertion of solid objects. Measurements were carried out and results agreed with the expectations from numerical solutions. The application of the sensor in this particular case study can greatly improve water conservation in public bathrooms and shopping centers. Moreover, its wireless functionality and ability to sense through non-metallic walls position it as a versatile tool for applications in the pharmaceutical, chemical, and food industries. The strategic use of array configuration, coupled with beam steering and advanced signal processing methods, heralds a promising future for the widespread adoption of such innovative sensors.

ACKNOWLEDGMENT

The authors thank Fatih Gerenli and the Eczacıbaşı team members for fruitful discussions on smart bathroom applications and further thank Eczacıbaşı for providing them with a sample of ceramic container.

REFERENCES

[1] K. D. Frederick and D. C. Major, "Climate change and water resources," *Climate Change*, vol. 37, pp. 7–23, 1997.
[2] N. W. Arnell, *Global Warming, River Flows and Water Resources*. Hoboken, NJ, USA: Wiley, 1996.
[3] D. P. Lettenmaier, A. W. Wood, R. N. Palmer, E. F. Wood, and E. Z. Stakhiv, "Water resources implications of global warming: A U.S. regional perspective," *Climate Change*, vol. 43, pp. 537–579, 1999.
[4] "www.Epa.Gov," Jun. 2014, Accessed: Oct. 18, 2023. [Online]. Available: https://www.epa.gov/watersense/residential-toilets#tab-3
[5] W. H. Smolinski, "Water saver toilet bowl flush," U.S. Patent 3758893, Sep. 18, 1973.
[6] S. Lunt, "Low flush toilet system," U.S. Patent 9399863 B2, Jul. 26, 2016.
[7] M. Henini and M. Razeghi, *Handbook of Infra-Red Detection Technologies*. Amsterdam, The Netherlands: Elsevier, 2022.
[8] Q. Jinping and L. Xingyun, "Toilet flushing device for intelligently recognizing urine and excrement," China Patent CN201850614U, Jun. 26, 2018.
[9] A. Cataldo, G. Monti, E. D. Benedetto, G. Cannazza, and L. Tarricone, "A noninvasive resonance-based method for moisture content evaluation through microstrip antennas," *IEEE Trans. Instrum. Meas.*, vol. 58, no. 5, pp. 1420–1426, May 2009.
[10] K. Sarabandi and E. S. Li, "Microstrip ring resonator for soil moisture measurements," *IEEE Trans. Geosci. Remote Sens.*, vol. 35, no. 5, pp. 1223–1231, Sep. 1997.
[11] L. Benkhaoua, M. T. Benhabiles, S. Mouissat, and M. L. Riabi, "Miniaturized quasi-lumped resonator for dielectric characterization of liquid mixtures," *IEEE Sensors J.*, vol. 16, no. 6, pp. 1603–1610, Mar. 2016.
[12] K.-C. Yoon, K.-G. Kim, J.-W. Chung, and B.-S. Kim, "Low-phase-noise oscillator using a high-QL resonator with split-ring structure and open-loaded T-type stub for a tumor-location-tracking sensor," *Appl. Sci.*, vol. 11, 2021, Art. no. 11550.
[13] A. M. Albishi, S. A. Alshebeili, and O. M. Ramahi, "Three-dimensional split-ring resonators-based sensors for fluid detection," *IEEE Sensors J.*, vol. 21, no. 7, pp. 9138–9147, Apr. 2021.
[14] L. Benkhaoua, S. Mouissat, M. T. Benhabiles, Y. Yakhlef, and M. L. Riabi, "Miniaturized planar resonator for bio-sensing field," in *Proc. 1st IEEE MTT-S Int. Microw. Bio Conf.*, 2017, pp. 1–3.

[15] E. C. Brdette, F. L. Cain, and J. Seals, "In vivo prove measurement technique for determining dielectric properties at VHF through micorowave frequencies," *IEEE Trans. Microw. Theory Techn.*, vol. 28, no. 4, pp. 414–427, Apr. 1980.
[16] E. Yildiz and M. Bayrak, "A different method determining dielectric constant of soil and its FDTD simulation," *Math. Comput. Appl.*, vol. 8, pp. 303–310, 2003.
[17] A. Al-Fraihat, A. Al-Mufti, U. Hashim, and T. Adam, "Potential of urine dielectric properties in classification of stages of breast carcinomas," in *Proc. 2nd Int. Conf. Electron. Des.*, 2014, pp. 305–308.
[18] M. Saadat-Safa, V. Nayyeri, A. Ghadimi, M. Soleimani, and O. M. Ramahi, "A pixelated microwave near-field sensor for precise characterization of dielectric materials," *Sci. Rep.*, vol. 9, 2019, Art. no. 13310.
[19] M. H. Zarifi and M. Daneshmand, "Wide dynamic range microwave planar coupled ring resonator for sensing applications," *Appl. Phys. Lett.*, vol. 108, 2016, Art. no. 232906.
[20] M. H. Zarifi, T. Thundat, and M. Daneshmand, "High resolution microwave microstrip resonator for sensing applications," *Sensors Actuators*, vol. 233, pp. 224–230, Sep. 2015.
[21] A. A. M. Bahar, Z. Zakaria, M. K. M. Arshad, A. A. M. Isa, Y. Darsil, and R. A. Alahnomi, "Real time microwave biochemical sensor based on circular SIW approach for aqueous dielectroc detection," *Sci. Rep.*, vol. 9, 2019, Art. no. 5467.
[22] W. Withayachumnankul, K. Jaruwongrungseeb, A. Tuantranont, C. Fumeaux, and D. Abbotta, "Metamaterial-based microfluidic sensor for dielectric characterization," *Sensors Actuators*, vol. 189, pp. 233–237, Jan. 2013.
[23] Z. Abbasi, M. Baghelani, M. Nosrati, A. Sanati-Nezhad, and M. Daneshmand, "Real-time non-contact integrated chipless RF sensor for disposable microfluidic applications," *IEEE J. Electromagn., RF Microw. Med. Biol.*, vol. 4, no. 3, pp. 171–178, Sep. 2020.
[24] J. G. D. Oliveira, J. G. D. Junior, E. N. M. G. Pinto, V. P. S. Neto, and A. G. D'Assunção, "A new planar microwave sensor for building materials complex permittivity characterization," *Sensors*, vol. 20, 2020, Art. no. 6328.
[25] A. Soffiatti, Y. Max, S. G. Silva, and L. M. D. Mendonça, "Microwave metamaterial-based sensor for dielectric characterization of liquids," *Sensors*, vol. 18, 2018, Art. no. 1513.
[26] M. Ozturk, U. K. Sevim, O. Akgol, E. Unal, and M. Karaaslan, "Determination of physical properties of concrete by using microwave nondestructive techniques," *ACES J.*, vol. 33, pp. 265–272, 2018.
[27] M. T. Islam, M. N. Rahman, M. S. J. Singh, and M. Samsuzzaman, "Detection of salt and sugar contents in water on the basis of dielectric properties using microstrip antenna-based sensor," *IEEE Access*, vol. 6, pp. 4118–4126, 2018.
[28] M. H. Zarifi and M. Daneshmand, "Liquid sensing in aquatic environment using high quality planar microwave resonator," *Sensors Actuators B*, vol. 225, pp. 517–521, 2015.
[29] M. H. Zarifi and M. Daneshmand, "Monitoring solid particle deposition in lossy medium using planar resonator sensor," *IEEE Sensors J.*, vol. 17, no. 23, pp. 7981–7989, Dec. 2017.
[30] M. H. Zarifi, M. Rahimi, and M. Daneshmand, "Microwave ring resonator-based non-contact interface sensor for oil sands applications," *Sensors Actuators B*, vol. 224, pp. 632–639, 2016.
[31] N. Nguyen-Trong and C. Fumeaux, "Tuning range and efficiency optimization of a frequency-reconfigurable patch antenna," *IEEE Antennas Wireless Propag. Lett.*, vol. 17, no. 1, pp. 150–154, Jan. 2018.
[32] D. M. Pozar, *Microwave Engineering*. Hoboken, NJ, USA: Wiley, 2012, pp. 228–271.
[33] C. A. Balanis, *Antenna Theory Analysis and Design*. Hoboken, NJ, USA: Wiley, 2016, pp. 783–873.
[34] F. Ghaderinezhad et al., "Sensing of electrolytes in urine using a miniaturized paper-based device," *Sci. Rep.*, vol. 10, 2020, Art. no. 13620.
[35] K. Wignarajah, E. Litwiller, J. W. Fisher, and J. Hogan, "Simulated human feces for testing human waste processing technologies in space systems," in *Proc. 36th Int. Conf. Environ. Syst.*, Jul. 2006, p. 9, doi: 10.4271/2006-01-2180.
[36] K. Nörtemann, J. Hilland, and U. Kaatze, "Dielectric properties of aqueous NaCl solutions at microwave frequencies," *J. Phys. Chem. A*, vol. 101, pp. 6864–6869, 1997.
[37] A. Stogryn, "Equations for calculating the dielectric constant of saline water (correspondence)," *IEEE Trans. Microw. Theory Techn.*, vol. 19, no. 8, pp. 733–736, Aug. 1971.
[38] J. B. Hubbard, L. Onsager, W. M. V. Beek, and M. Mandel, "Kinetic polarization defficiency in electrolyte solutions," *Proc. Nat. Acad. Sci. USA*, vol. 74, no. 2, pp. 401–404, 1977.
[39] J. A. Lane and J. A. Saxton, "Dielectric dispersion in pure polar liquids at very high radio frequencies. III. The effect of electrolytes in solution," *Proc. Roy. Soc. Lond. A, Math. Phys. Sci.*, vol. 214, no. 1119, pp. 531–545, 1952.
[40] V. Kumar, J. V. Dhabalia, G. G. Nelivigi, and M. S. Punia, "Age, gender, and voided volume dependency of peak urinary flow rate and uroflowmetry nomogram in the Indian population," *Indian J. Urol.*, vol. 25, pp. 461–466, 2009.
[41] R. Salmon, "Introduction to Ocean Waves," Scripps Inst. Oceanography, Univ. California, San Diego, CA, USA.
[42] "Vitra." Accessed: May 24, 2024. [Online]. Available: https://www.vitra.co.uk/flushingsolutions-flush-plates/concealed-frame-systems/
[43] J. Leonard, "medicalnewstoday," May 2024. Accessed: May 24, 2024. [Online]. Available: https://www.medicalnewstoday.com/articles/321461
[44] S. A. Walter, L. Kjellstrom, H. Nyhlin, N. J. Talley, and L. Agréus, "Assessment of normal bowel habits in the general adult population: The Popcol study," *Scand. J. Gastroenterol.*, vol. 45, pp. 556–566, 2010.

SOBHAN GHOLAMI received the undergraduate degree from Marmara University, Istanbul, Türkiye, in 2021. He was an undergraduate Researcher with the bioMEMs Laboratory, Department of Electrical and Electronics Engineering, Marmara University. He joined the Department of Electrical and Electronics Engineering, Bilkent University, Ankara, Türkiye, in 2021, as a Research Graduate Student. His research interests include electromagnetic theory and application, antenna/microwave theory and measurement.

EMRE UNAL received the B.Sc. degree in electrical and electronics engineering from Hacettepe University, Ankara, Türkiye, in 2005. He is currently a full-time Research Engineer with the Institute of Materials Science and Nanotechnology, Bilkent University, Ankara, under the supervision of Prof. H. V. Demir, where he is working on the development of microwave and optoelectronic devices.

HILMI VOLKAN DEMIR (Fellow, IEEE) received the B.Sc. degree in electrical and electronics engineering from Bilkent University, Ankara, Türkiye, in 1998, and the M.Sc. and Ph.D. degrees in electrical engineering from Stanford University, Stanford, CA, USA, in 2000 and 2004, respectively. In 2004, he joined Bilkent University, where he is currently a Professor with joint appointments with the Department of Electrical and Electronics Engineering, Department of Physics and Institute of Materials Science and Nanotechnology (UNAM). He is also a Fellow of the National Research Foundation in Singapore and Professor with Nanyang Technological University, Singapore. His research interests include the development of innovative optoelectronic and RF devices. He is a member of the Turkish Academy of Science.